Materials Physics and Mechanics 44 (2020) 34-47 Received: January 28, 2018

DEPOSITION KINETICS AND BOUNDARY LAYER THEORY IN THE CHEMICAL VAPOR DEPOSITION OF β-SiC ON THE SURFACE OF C/C COMPOSITE

H. Aghajani[1*], N. Hosseini[1], B. Mirzakhani[2]

[1]Department of Materials Engineering, University of Tabriz, Tabriz, Iran

[2]Faculty of Engineering, Arak University, Arak, Iran

*e-mail: h_aghajani@tabrizu.ac.ir

Abstract. In this study, SiC was deposited on carbon/carbon (C/C) composite substrate using chemical vapor deposition (CVD) method to investigate the kinetics of the deposition process. Therefore, the time, temperature, precursor composition ($SiCl_4$:N_2:CH_4) and substrate position in the reactor were varied to evaluate the deposition rate. X-ray diffraction (XRD) method was used to characterize the phase composition and calculate the grain size and the texture coefficient of the coatings. Field emission scanning electron microscopy (FESEM) was utilized to observe the coating morphology, microstructure and thickness. As observed β-SiC was the dominant phase of the coating with varied preferred growth crystalline planes of (111), (220) or (311). The coating thickness was 2 μm and 5 μm for the samples treated at 1000 and 1100ºC, respectively.

Keywords: chemical vapor deposition, boundary layer, deposition rate, SiC coating, C/C composite

1. Introduction

Carbon/carbon (C/C) composites have recently attracted much interest due to their unique physical, mechanical and chemical properties. Some advantageous properties such as low weight, good high-temperature strength, high thermal conductivity, resistance to thermal shock and resistance to high-temperature erosion make C/C composites more useful [1-6]. The most important defect of these composites is oxidation at temperatures higher than 500ºC, which could be prevented by applying an appropriate coating on them. Silicon carbide (SiC) is the most applicable coating for C/C composites due to the low thermal expansion coefficient and high adhesion between coating and the substrate [7-12]. Chemical vapor deposition (CVD) is an attractive and efficient coating method for applying SiC coating on C/C composite. This method is based on the decomposition of a gaseous reactant in an activated environment and the formation of solid products. The thermodynamics and kinetics of CVD process could be used for identification of the process and reactions. Thermodynamic calculations could be employed to investigate the feasibility of the reaction, while kinetics study could be used to determine the controlling factor in deposition procedure. To obtain a uniform coating with a certain morphology and expected properties, an exhaustive investigation should be carried out on the deposition process to determine the controlling factors [13-18]. The aim of this research is to study the relationship between boundary layer theory and deposition kinetics of β-SiC coating on a C/C composite by CVD method. Therefore, the influences of various parameters on the deposition rate were studied.

http://dx.doi.org/10.18720/MPM.4412020_5

2. Material and methods

C/C 2D bi-directional structured samples was obtained from Jiao company. The modulus of elasticity, thermal conductivity and density of the composite were about 180 GPa, 100 W/m·K and $1.8 \cdot 10^3$kg/m³, respectively. Cubic specimens with dimensions of 10 mm×10 mm×10 mm were cut from the bulk C/C composite by means of wire-cutting method. The samples were ground with emery silicon carbide papers of 400-1300 grits. Thereafter, the ground specimens were cleaned ultrasonically in acetone and ethanol for 15 min followed by drying in the oven at 200ºC for 2 h. Low pressure chemical vapor deposition (LPCVD) process was carried out by means of a setup with horizontal reactor (NSSG, Iran).The deposition was performed using pure $Sicl_4$ (Merck, Germany) and CH_4 as well as N_2 as dilution and carrier gas. The schematic diagram of the CVD setup is shown in Fig. 1.

To evaluate the deposition rate, deposition parameters varied as follows; temperature: 900, 1000 and 1100ºC, time: 1, 2 and 3 h, $SiCl_4$:N_2:CH_4: 2:100:100, 4:100:100 and 6:100:100 (sccm). Furthermore, the samples were deposited at different positions in the reactor to study the effect of sample position.

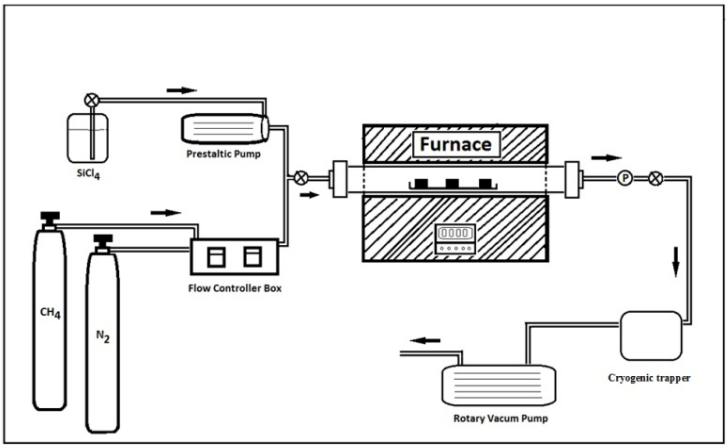

Fig. 1. The schematic diagram of the CVD setup

Deposition rate of the SiC coating were calculated utilizing the following equation:

$$R = \frac{W - W_0}{A.\,t}, \tag{1}$$

where, W_0 and W are the weight of the sample before and after CVD process, respectively, A is the sample surface area and t is the deposition time.

X-ray diffraction (XRD) (Bruker, Germany, Cu K_α=1.54 Å) was used to characterize the phase composition and measure the grain size and texture of the coatings. Field emission scanning electron microscopy (FESEM) (Tescan, Czech Republic) was utilized to measure the thickness and investigate the morphology of the coatings.

3. Results and discussion

X-ray diffraction analysis. Figure 2 illustrates XRD pattern of SiC coating applied on a C/C composite by CVD method. It can be seen that β-SiC is the major phase of the coating and also one carbon peak is observable.

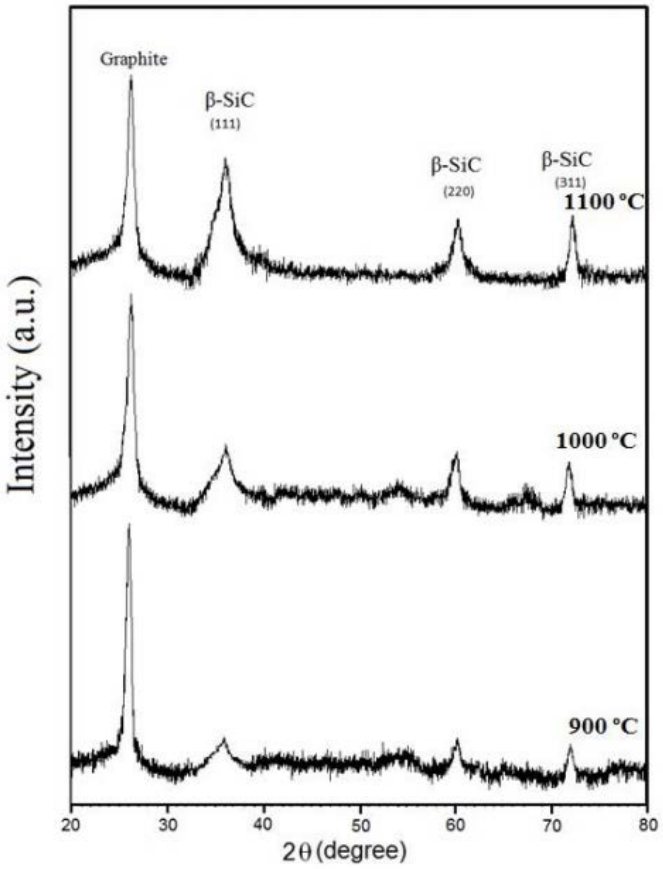

Fig. 2. XRD pattern of β-SiC coating applied on C/C composite by CVD method

The intensity of the carbon peak for the coatings produced at 1100ºC is lower than that of the coatings produced at 900 and 1000ºC. This carbon peak is related to the C/C substrate as X-ray beam can penetrate through 30 μm thick coatings [19]. As can be seen in FESEM cross-sectional images (Fig. 3), the thickness of the coatings produced at 1000 and 1100ºC was about 3 and 5 μm, respectively. Therefore, the carbon peak rises from substrate. Furthermore, with increasing deposition temperature, the intensity of β-SiC diffraction peaks enhanced. From the X-ray diffraction patterns, the texture coefficient (TC) of the coatings could be measured. The TC represents texture and preferred orientation of the crystal surface. The lower the TC value for certain (h k l) plane, the weaker the growth for that plane and vice versa. The TC and preferred growth orientation depend on the deposition conditions and on the deposition kinetics. The TC of (111), (220) and (311) crystal planes in polycrystalline SiC coating can be calculated using Harris method [19-20]:

$$TC = \frac{I_i / I_0}{(1/n) \times \sum_{i=1}^{n} (I_i / I_0)}, \tag{2}$$

where, I_i is the measured relative intensity of a (h k l) plane and I_0 is the standard intensity of the plane (taken from ASTM standard intensities) and n is the number of reflections. TC values for (111), (200) and (311) crystalline planes are shown in Fig. 4. It can be observed that at 900 and 1000ºC, the TC of (200) and (311) is higher than (111) plane. At 1100ºC, the TC of (111) direction is higher than that of (220) and (311). Hence, with increasing temperature, preferred orientation changes from (220) and (311) to (111) and at higher temperatures β-SiC tends to grow through densely-packed atomic planes.

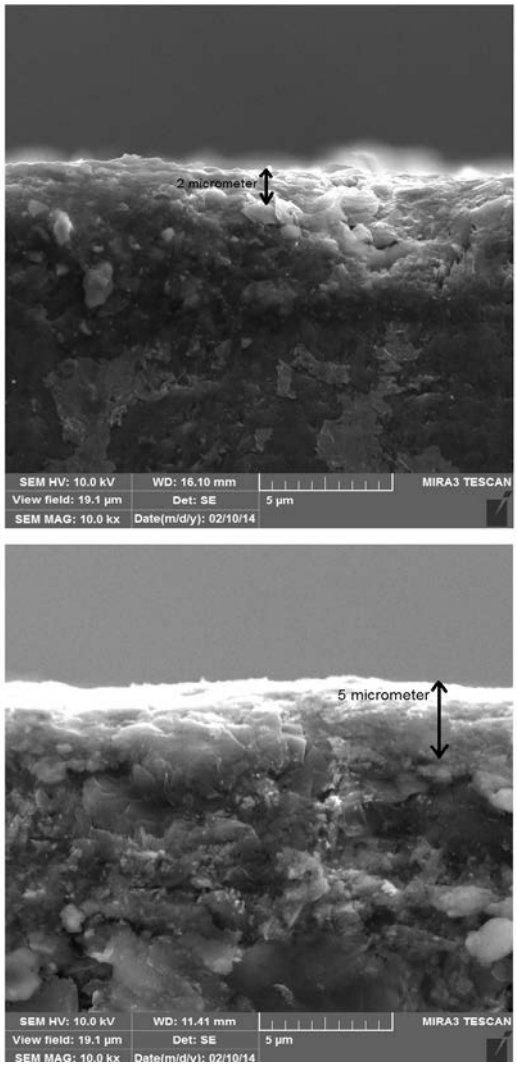

Fig. 3. Cross section of SiC coated C/C at different temperatures of 1000 and 1100ºC

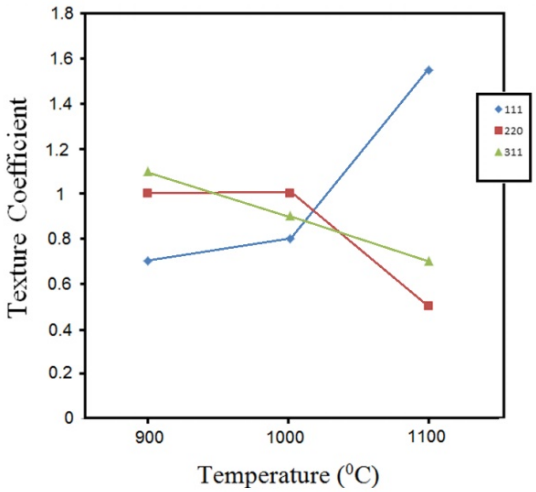

Fig. 4. Texture coefficients of β-SiC coating at different temperatures

The SiC coating grain size was calculated using the Debye-Scherer formula, as given in Equation (3) [21]:

$$D = \frac{0.9\lambda}{\beta \cos\theta}, \quad (3)$$

where, D is the grain size of the crystallite, λ is the wavelength of the incident X-ray, β is the width of peak in the middle of maximum intensity and θ is the related point on the horizontal axis. Table 1 presents the average crystal size of the SiC coating deposited at different temperatures. As it can be seen, the grain size of coating increases from 70 to 350 nm as the deposition temperature increases from 900 to 1100ºC.

Table 1. Calculated average grain size of coating at different temperatures

Deposition temperature (ºC)	Average grain size (nm)
900	70
1000	145
1100	350

Effects of different parameters on deposition kinetics. In general, the CVD process involves the following seven key steps [22]:

1. Transport of gaseous species in to the reactor.
2. Formation of intermediate species from reactant gaseous species.
3. Diffusion of intermediate species through the boundary layer to the substrate surface.
4. Adsorption of these species on the surface.
5. A single-step or multi-step reactions on the substrate surface.
6. Desorption of by-product species from the substrate.
7. Forced exit of un-reacted gases and by-product species from the reactor.

The schematic illustration of CVD steps during the deposition is shown in Fig. 5. Steps (1) and (7) are mass transport-controlled processes. Rate of step (1) is controlled by experimental conditions and flow rate of the precursors in the reactor. In addition, step (7) is controlled by the gas flow rate in the reactor and the power of vacuum systems. Step (5) is consisting of the intermediate gas reaction in the surface. Steps (3) and (6) show mass transport through the boundary layer. The rate of these steps can be determined by Fick's first law. In general, the steps in this model can be classified into two categories; the mass-transport-controlled steps (1, 3, 6 and 7) and the surface-reaction-controlled steps (2, 4 and 5). Amongst, the slowest step determines either the process is a mass-transport or surface-reaction controlled [18,22]. Thus, various parameters were studied to determine the kinetics of coating process.

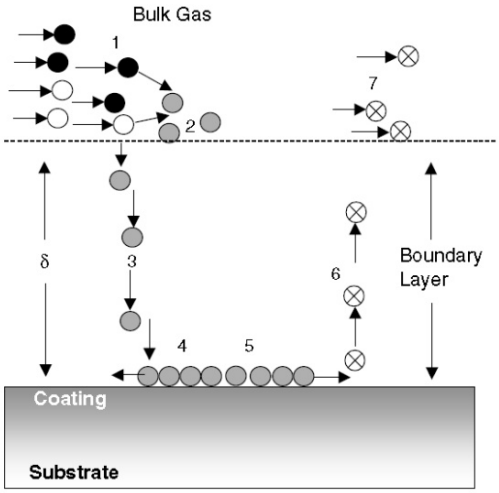

Fig. 5. Schematic diagram of the mechanistic steps of CVD process [20]

Temperature. Figure 6 illustrates the deposition rate of coating as a function of temperature. It can be seen that the deposition rate increases with deposition temperature due to overcoming the thermodynamically-formed barriers. However, at elevated temperatures, the consumption rate of the reactants at the surface of furnace hot wall is high too and it has a destructive effect on the deposition rate which can be clearly seen in Fig. 6. Thus, increasing the deposition temperature can be assumed as a positive and negative factor in SiC deposition.

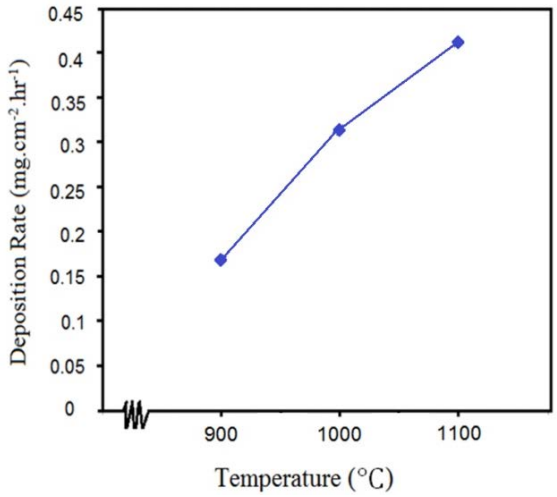

Fig. 6. Deposition rate of coating versus temperature

For determination of deposition kinetics in CVD process, an accurate knowledge of boundary layer is necessary. According to boundary layer theory [11], mass transport through boundary layer could be pursued utilizing Fick's first law [22].

$$J_A = -\frac{D_{AB}}{RT}\frac{dC_A}{dx}, \tag{4}$$

where, J_A is the diffusion flux of specie A, D_{AB} is diffusivity of reactants, C_A is concentration of specie A, R is gas constant, T is temperature and x is the direction perpendicular to the substrate surface. In boundary layer theory of a CVD process, x is the thickness of boundary layer. The average boundary layer thickness as a function of temperature is given as [22]:

$$\delta = \frac{10}{3}\sqrt{\frac{L\mu_{mix}}{\rho u}}, \tag{5}$$

where, L is the length of the substrate, μ_{mix} is the viscosity of the gas mixture, ρ and u are the density of the gas and the linear velocity of the gas in reactor, respectively. The density and velocity of the gas are function of temperature. The density is estimated by ideal gas law and the viscosity is estimated by some models [23]. Calculated results of the average boundary layer are shown in Fig. 7. As it is illustrated, an increase in temperature causes an increase in the thickness of boundary layer. Increasing the temperature causes the viscosity enhancement of the gas in reactor. With increasing gas concentration, the velocity of reactants in the reactor decreases. Thus, according to Eq. 5, the boundary layer will get thicker. With more thickening of the boundary layer, the growth kinetics will be controlled by mass transport. When the deposition rate is controlled by mass transport, the particles pass through the boundary layer thickness and reach to the substrate surface and the coating has enough time to grow. As can be seen in Fig. 4, the preferred orientation for growth of the crystals at high temperatures is (111) crystalline plane. Thus, it can be concluded that at elevated temperatures, the boundary layer thickness increases and the deposition process is controlled

by mass transfer. Due to having enough time for being ordered, crystals grow in high density orientation.

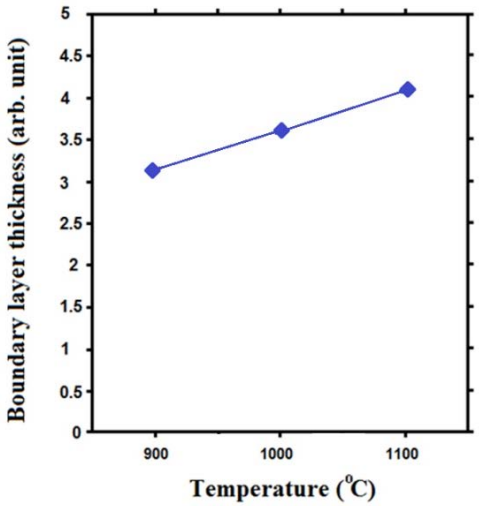

Fig. 7. Calculated boundary layer thickness at different temperatures

Precursor composition. The effect of composition of precursor on deposition rate of coating is shown in Fig. 8. The results indicate that the deposition rate increases with increasing the amount of $SiCl_4$ in the gas composition. Increasing $SiCl_4$ as precursor from 2 to 4 sccm has a meaningful effect on deposition rate, but increasing it from 4 to 6 sccm has a lower effect on deposition rate. When $SiCl_4$ amount is 2 sccm, the concentration of active particles containing Si is very low in comparison to the active particles containing C, thus the deposition rate is very low. With increasing $SiCl_4$ up to 4 sccm, the concentration of Si-containing particles on the surface increases and the deposition rate increases severely. However, with increasing $SiCl_4$ content up to 6 sccm, the deposition rate slightly increases. In this case, the excessive concentration is the controlling factor of the deposition process.

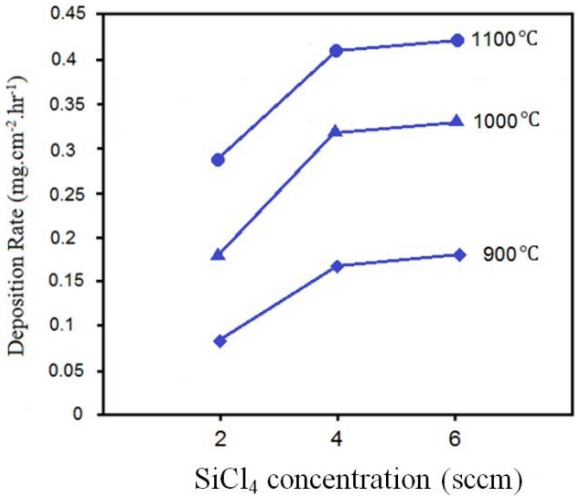

Fig. 8. Deposition rate of SiC coating versus $SiCl_4$ concentration

Time. The deposition time is one of the most important and controlling parameters in the nucleation and growth of SiC on C/C composite. Figure 9 shows the effect of time on deposition rate of SiC coatings. It can be seen that the deposition rate is low at first hour, followed by a significant increase especially when the deposition time increased to 3 hours. When the deposition time is low, SiC nucleates on the surface of C/C composite.

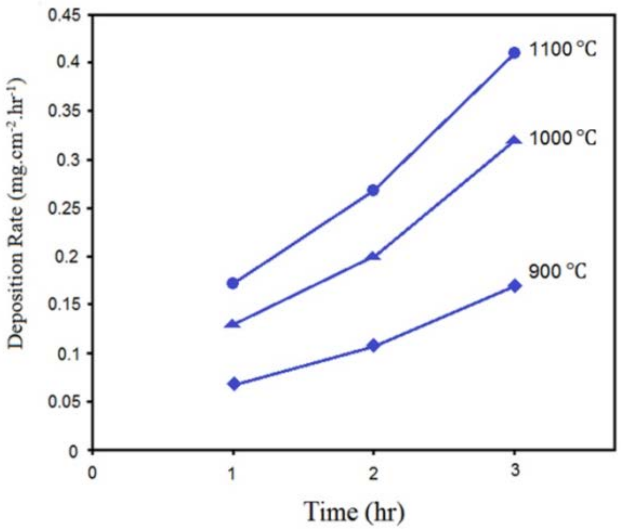

Fig 9. Deposition rate of SiC coating versus deposition time

Position of the samples in the reactor. Position of substrate in the CVD reactor is one of the effective parameters on deposition rate. In different parts of the reactor, temperature, pressure and gas flow input is sometimes different. Figure 10 illustrates substrate positioning in the CVD reactor and its effects on deposition rate. As it is obvious, the deposition rate is higher in position 2 than that in positions 1 and 3. Thermocouples of the CVD reactor furnace are located close to this location and displayed temperature is the temperature of this position. In this position, since the distance from the inlet and outlet of reactor is high, the temperature is higher and mass transfer is easier. Thus, the activated particles suspended in the reactor react readily on the substrate surface. However, around position (1) and (3) due to the closeness to input and output gates, the temperature is lower and the deposition rate is less.

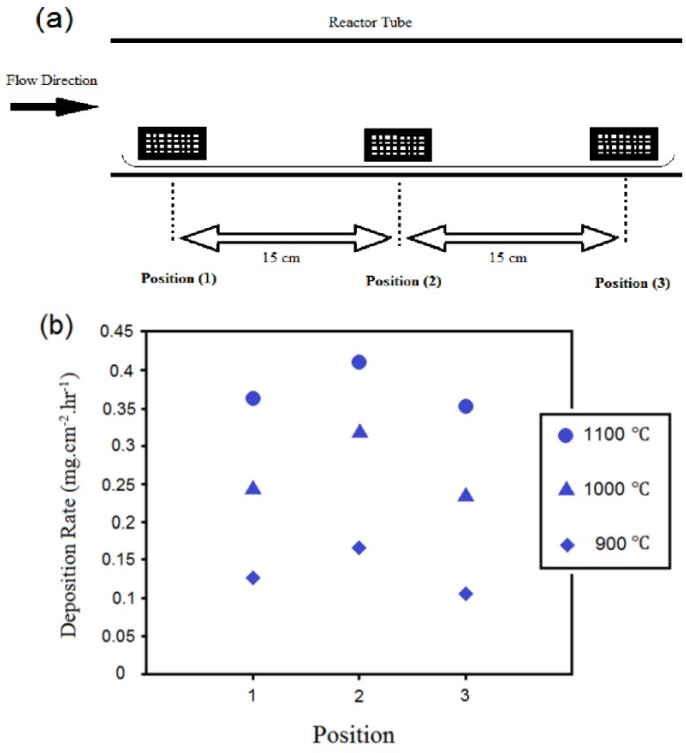

Fig. 10. (a) Schematic illustration of substrate position in reactor, (b) deposition rate of SiC coating versus substrate position

Controlling factors of deposition. To determine the factors controlling the deposition rate, its changes versus temperature is plotted in Fig. 11. The resulted curve can be divided into two regions. Due to the changes in region (a), the slope of the curve is constant, but in region (b), a noticeable decrease of the slope could be clearly seen. From the calculated slope, it could be noted that chemical reactions, mass transfer and surface migration, network integration and byproducts desorption from surface are the controlling factors in region (a). The surface processes strongly depend on deposition temperature and the processes speed up with temperature enhancement. Also, it could be mentioned that deposition could be controlled by mass transport of the activated particles in the boundary layer in region (b). Hence, there is a limitation in mass transport and deposition rate, which are slightly dependent on temperature. In fact, at high temperatures, surface processes are accelerating, thus fewer particles could reach the surface. Therefore, the growth mechanism of the deposit also changes. The change in mechanism of the crystal growth was also observed by calculation of the preferred orientation of crystals. The (111) crystalline plane is more compact than (220) and (311) crystalline planes and Si and C atoms, are arranged in this plane in compressed mode. It can be concluded that, at low temperatures, deposition is controlled by chemical reaction and particles can easily reach the surface at lower speeds. When the surface reaction is carried out at lower speeds, the particles deposit in irregular form and may be stacked with little compression. In this state, the texture coefficient (TC) of (220) and (311) planes are more than that of (111). When the deposition rate is controlled by mass transport, the transfer of activated particle to surface is done slower and atoms have adequate time to be arranged and compressed. The crystals grow in plane (111) with the lowest surface energy. Certainly, there is a little information about the details of the surface process mechanisms, but the relationship between temperature and activation energy can be defined by the following Arrhenius formula [18]:

$$R = A\exp\left(-\frac{E_a}{RT}\right), \tag{6}$$

where E is the activation energy, A is a constant; R and T are the gas constant and temperature, respectively. The activation energy could be obtained from the slope of the Fig. 11. Results of the activation energy calculation showed that the activation energies in regions (a) and (b) are 69 kj.mol^{-1} and 18 kj.mol^{-1}, respectively.

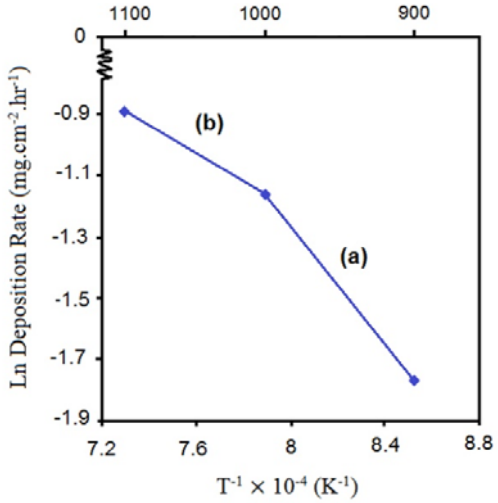

Fig. 11. The deposition rate curve versus inverse temperature

Region (a) represents a region that is controlled by chemical reaction and the activation energy in this area is much greater. The high activation energy indicates that deposition takes

place with difficulty and barriers ahead of deposition process are high. Therefore, it is expected that the formed coating has a low thickness. In region (b), the activation energy is lower. Deposition has a lower dependence on temperature in this region. Hence, SiC deposits more easily.

FESEM images of coatings. Figure 12 demonstrates surface morphology of C/C composite before and after SiC deposition. As it is observed, C/C has a laminate configuration due to the flake-like structure of C/C, which acts as a template for further SiC growth. As it is seen from the figure, SiC crystals grow according to flakes of the substrate and are not capable of growing on the surface porosities of C/C surface. Therefore, deposition time needs to be extended. On the other hand, since the temperature is an effective parameter, it also needs to be elevated to prepare adequate energy for SiC particles to grow in porosities.

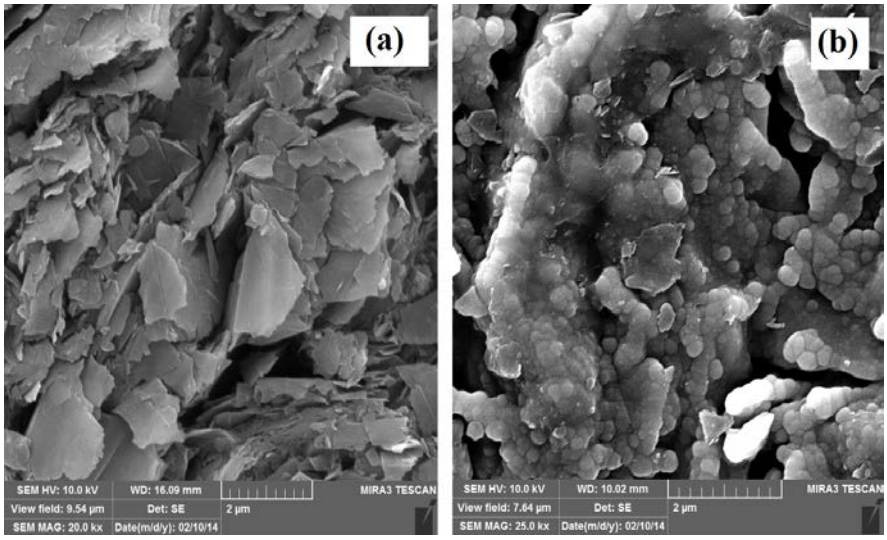

Fig. 12. Surface morphology of C/C composite (a) before and (b) after SiC deposition

Figure 13 presents EDS analysis of SiC coating. As it is seen, the coating is consisted of high percentage of C and Si. Presence of O in composition of coating indicates that some areas of SiC have undergone oxidation. However, as the amount of oxygen is low, oxidation cannot be widespread on the coating.

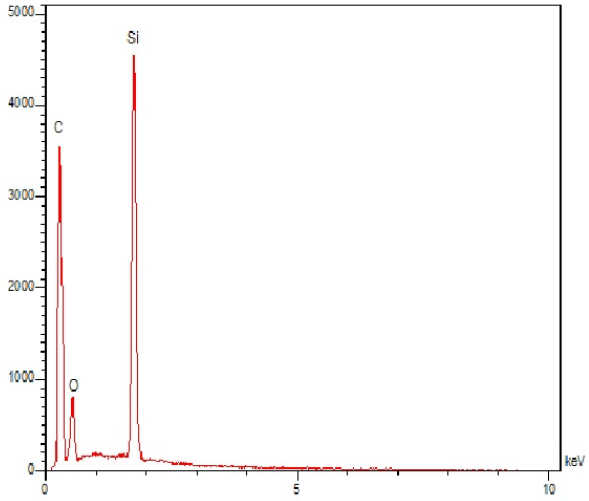

Element	W%
C	47.65
O	8.44
Si	43.91

Fig. 13. EDS analysis of SiC coating on C/C substrate

Figure 14 shows FESEM images of SiC-coated C/C with two different magnifications. As it is observed, at 900 and 1000ºC, the generated clusters are very small and by increasing temperature, they start to grow and become bigger and bigger. At 1100ºC, many crystals could grow and in some cases, crystal size has even reached 300 μm.

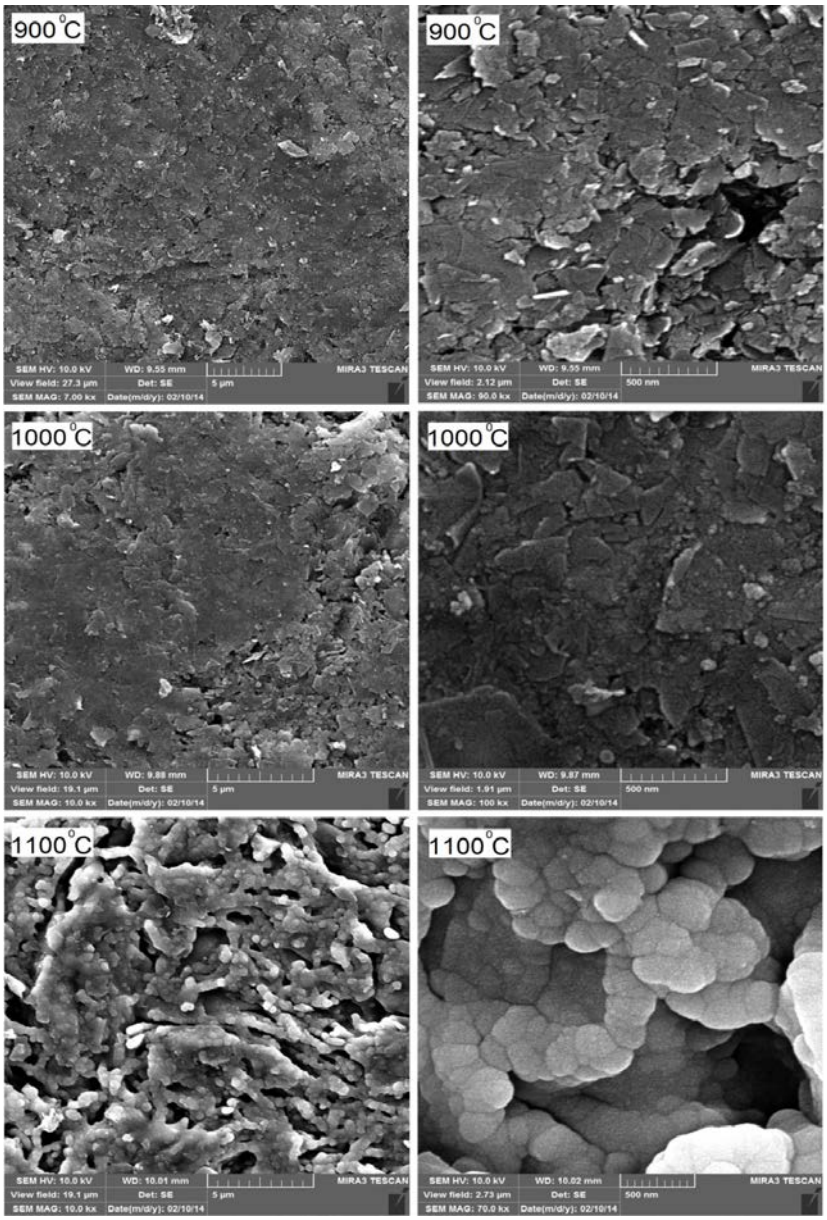

Fig. 14. FESEM images of SiC coated C/C with two different magnifications at 900 and 1000ºC

Effect of deposition time on growth morphology of coating. Figure 15 presents FESEM images of the applied SiC coating in different periods of times. As it is observed, by increasing deposition time, the crystallized grains on the surface of C/C have grown and their size have increased. When the deposition time is less, crystals nucleate and if they reach critical radius, begin to grow. As can be observed in the figure, during 1 h, small particles have been generated on the surface of the composite. By increasing deposition time up to 2 h, the same particles exist on the surface. However, they had the sufficient time to absorb more Si and C atoms to be enlarged and reach the diameter of 100 nm. When the time was further

allocated, initial nucleation and growth both occurred at the first hour of deposition. However, the main growth happened at the last hour of deposition and crystals have been able to reach themselves to the diameter of 200 to 300 nm homogeneously. From above mentioned discussion, it is concluded that SiC crystals grow in an Island-type manner.

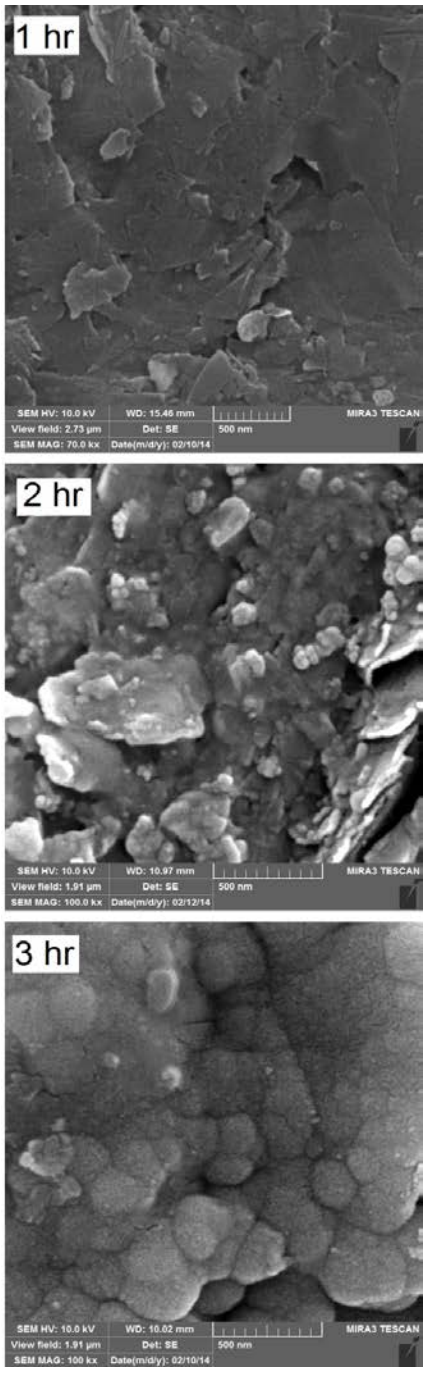

Fig. 15. FESEM images of the applied SiC coatings in different periods of times

4. Conclusions

From the above-mentioned results, the following conclusions could be drawn;

1) Phase characterization of SiC coating applied at different temperatures shows that the β-SiC phase in crystalline planes (111), (200) and (311) grows on the surface of C/C composite and the phase peak intensity increases with increasing temperature.

2) Texture coefficient calculation results using XRD analysis revealed that crystal preferential orientation at 900 and 1000ºC were (311) and (200) and at 1100ºC, preferred orientation of crystalline plane was (111).

3) Grain size calculation by utilizing XRD analysis revealed that grain size of the coating applied at 900, 1000 and 1100ºC were 70, 145 and 350 nm, respectively.

4) With increasing temperature, the amount of $SiCl_4$ in precursor, and placement of sample in middle position of reactor, deposition rate of SiC on C/C composite increases.

5) Kinetics studies show that at 900 and 1000ºC, controlling factor is the chemical reaction and at 1100ºC, it is mass transport.

Acknowledgements. *No external funding was received for this study.*

Reference

[1] Pierre D. *Fibers and Composites, World of Carbon.* France: Taylor & Francis Routledge; 2003; 2.

[2] Inagaki M. *New Carbons: Control of structure and Functions*. Japan: Elsevier Science Ltd; 2000.

[3] Burchell TD. *Carbon materials for advanced Technologies.* USA: Elsevier Science Ltd; 1999.

[4] Luo R, Liu T, Li J, Zhang H, Chen Zh, Tian G. Thermophysical properties of carbon/carbon composites and physical mechanism of thermal expansion and thermal conductivity. *Carbon*. 2004;42: 2887-2895.

[5] Liu H, Jin Zh, Haob Zh, Zeng X. Improvement of the mechanical properties of two-dimensional carbon/carbon composites. *Materials Science and Engineering: A.* 2008;483: 316-318.

[6] Tzeng Sh Sh, Pan JH. Densification of two-dimensional carbon/carbon composites by pitch impregnation. *Materials Science and Engineering: A.* 2001;316: 127-134.

[7] Bacos MP. Carbon-carbon composites: oxidation behavior and coatings protection. *Journal of Physics.* 1993;3: 1895-1903.

[8] Strife JR. Protective Coating for Carbon-Carbon Composites. In: ASM Handbook *Surface Engineering*. 1994; 5. p. 2337-2347.

[9] Don J, Wright MA, He J. *Investigation of Oxidation protection Systems for Carbon-Carbon Composites: formed by chemical vapor deposition and plasma-assisted chemical vapor deposition technique.* Airf. Office of Scientific Research. 1991; 122.

[10] Kravetskii GA, Firsova TD, Kolesnikov SA. Composite Refractory Protective Coatings for Carbon-Graphite Materials. *Refractories and Industrial Ceramics.* 2008;49: 455-460.

[11] Zhao J, Wang G, Guob Q, Liu L. Microstructure and Property of Sic Coating for Carbon Materials. *Fusion Engineering and Design.* 2007;82: 363-368.

[12] Xin Y, Qi-zhong H, Yan-hong Z, Xin C, Zhe-an S, Ming-yu Z, Zhi-yong X. Anti-Oxidation Behavior of Chemical Vapor Reaction SiC Coatings on Different Carbon Materials at High Temperatures. *Transactions of Nonferrous Metals Society of China.* 2009;19: 1044-1050.

[13] Pierson HO. *Handbook of Chemical Vapor Deposition (CVD): Principles, Technology, and Applications*. New Mexico: Noyes Publications/William Andrew Pub.; 1999.

[14] Spear KE. Principles and applications of chemical vapor deposition (CVD). *Pure and Applied Chemistry.* 1982;54: 1297-1311.

[15] Rees WSJr. *CVD of Nonmetals*. New York; VCH; 1996.

[16] Jones AC, Hitchman ML. *Chemical Vapor Deposition: Precursors, Processes and Applications*. Glasgow: Royal Society of Chemistry; 2008.

[17] Yan Y, Weigang Zh. Kinetic and microstructure of SiC deposited from SiCl4-CH4-H2. *Chinese Journal* of *Chemical Engineering.* 2009;17: 419-426.
[18] Choy KL. Chemical vapour deposition of coatings, *Progress in Materials Science.* 2003;48: 57-170.
[19] Long Y, Javed A, Chen ZK, Xiong X, Xiao P. Deposition Rate, Texture, and Mechanical Properties of SiC Coatings Produced by Chemical Vapor Deposition at Different Temperatures. *International Journal* of *Applied Ceramic Technology*. 2013;10: 11-19.
[20] Liu R, Zhang C, Zhou X, Cao Y. Structural Analysis of Chemical Vapor Deposited β-SiC Coatings from CH3SiCl3-H2 Gas Precursor, *Journal of Crystal Growth.* 2004;270: 124-127.
[21] Cullity BD, Stock SR. *Elements of X-ray diffraction. 3rd ed.* USA: Prentice Hall; 2001.
[22] Park JH, Sudarshan TS. C*hemical Vapour Deposition, Surface Engineering Series, Vol. 2*. Ohio: ASM International; 2001.
[23] Poling BE, Prausnitz JM, Oconnell JP. *The Properties of Gases and Liquids, 5th ed.* New York: McGraw-Hill; 2004.